Food Engineering Progress
Vol. 5, No. 1. pp. 64~70 (2001년 2월)

Numerical Study of Fluid Flow and Heat Transfer in a Tunnel Oven for Bakery

Kwan-Gu Kang, Hong-Sun Ryou, Choong-Ik Kim, Dong-Soon Noh* and Ki-Bae Hong**

Department of Mechanical Engineering Chung-Ang University
**Korea Institute of Energy Research*
***Department of Thermal Engineering Chung-Ju National University*

Abstract

A numerical simulation has been carried out for the tunnel oven. In this computation, finite volume method is presented for the solution of the three-dimensional incompressible, steady Navier-Stokes equations based on a non-orthogonal coordinate with non-staggered variable arrangement. The accuracy of the numerical calculation were compared with experimental data and showed predictions of the velocity and temperature in the tunnel oven. Parametric studies are performed to determine the sensitivity of the temperature above the band to variations in oven conditions. The velocity of band had a negligible effect on the temperature of the oven, but capacity of suction was the most effective parameter on lateral temperature difference.

Key words: tunnel oven, simulation, band, suction

Introduction

Tunnel oven is widely used for bakery industry. But there was no much theoretical ground in manufacturing and designing the oven. Only skilled experts have designed the oven with experience and instinct. So to manufacture the oven, the analysis of temperature profile inside the oven is very important. Especially to make the temperature profile constant inside the oven is most important.

It is ideal to manufacture the tunnel oven through the experimental work for various conditions. But it costs high and takes much time to do experimental work for various condition. For optimum tunnel oven, it is desirable to make the simulation model based on the minimum experimental data and to develop the oven by using this model. This is because it is very cost-effective and easy to apply different condition for manufacturing tunnel oven.

Corresponding author: Hong-Sun Ryou, Professor, Department of Mechanical Engineering, Chung-Ang University, 221, Heuk-Seok Dong, Dong-Jak Gu, Seoul 156-756, Korea. (phone: +82-2-820-5280)

Kang *et al.* (1997) analyzed the tunnel oven assuming that the flow in the oven is laminar. But inside the oven, Reynolds number is high and it is more accurate method to analyze the tunnel oven assuming that the flow is turbulent. So we analyze the tunnel oven assuming that the flow in the tunnel oven is turbulent.

A typical configuration of tunnel oven is shown in Fig. 1. Uncooked biscuits are carried by a moving band through an tunnel oven equipped with ribbon burners. The direction of moving belt and the direction of ignition gas from cylindrical burners are the same. The suction dispels the ignition gas and moisture from the biscuits. The temperature of the ignition gas and band speed are maintained at product-specific values to ensure

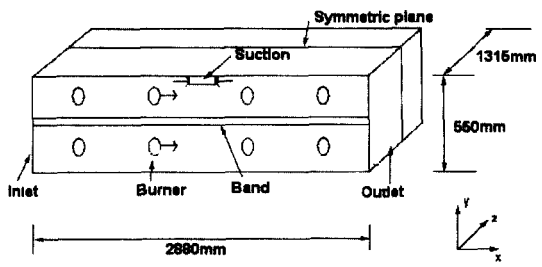

Fig. 1. Schematic of a typical tunnel oven.

the uniform quality.

The tunnel oven's thermal response is affected mostly by convective heat transfer modes. Surface-to-surface radiative exchange is ignored because temperature of surface is about 300°C and surface radiation is ignorable. In general, ignition gas is mixed due to the simultaneous presence of the moving band and suction-induced velocities. Conduction within the moving band is negligible. To design the oven efficiently and/or specify its operating conditions, it is necessary to predict and quantify the heat transfer rates within the oven. Hence, the objectives here are to (i) develop a numerical model capable of predicting the thermal response of band to specific oven conditions, (ii) demonstrate the models capability through presentation of sample result and (iii) make the data base to design the optimum oven by parametric study.

Governing Equations and Turbulent Modelling

Governing equations

Conservation of mass:

$$\frac{1}{J}\frac{\partial}{\partial_j}[J\alpha_m^j + (\rho U_m)] = 0 \tag{1}$$

Conservation of momentum:

$$\frac{1}{J}\frac{\partial}{\partial X_j}[J\alpha_m^j(\rho U_m U_j - \tau_{mi} + P\delta_{mi})] = 0 \tag{2}$$

Conservation of energy:

$$\frac{1}{J}\frac{\partial}{\partial X_j}\left[J\alpha_m^j\left(\rho U_m U_j - \gamma_{eff}\frac{\partial T}{\partial X_n} + \alpha_m^n\right)\right] = q^{'''m} \tag{3}$$

where U_m is Cartesian velocity component, and τ_{mi} is stress tensor. If y_i is cartesian coordinate and X^j is general coordinate, J is the Jacobian which transfers cartesian coordinate to the general coordinates.

Turbulence modeling

Turbulence kinetic energy:

$$\frac{1}{J}\frac{\partial}{\partial X^j}\left[J\alpha_m^j\left(\rho U_m k - \frac{\mu_t}{\sigma_g}\frac{\partial \varepsilon}{\partial X^n} + \alpha_m^n\right)\right] = P_k - \rho\varepsilon \tag{4}$$

Turbulence dissipation rate equation:

Table 1. Standard k–ε turbulence model constants

σ_k	σ_k	C_μ	C_1	C_2
1.0	1.3	0.09	1.44	1.92

$$\frac{1}{J}\frac{\partial}{\partial X^j}\left[J\alpha_m^j\left(\rho U_m \varepsilon - \frac{\mu_t}{\sigma_\varepsilon}\frac{\partial \varepsilon}{\partial X^n} + \alpha_m^n\right)\right] = \frac{\varepsilon}{k}(C_1 P_k - C_2\rho\varepsilon) \tag{5}$$

where P_k is turbulent energy source term and is defined.:

$$P_k = m_t\left[\frac{\partial U_i}{\partial X^n}\alpha_j^n + \frac{\partial U_j}{\partial X^m}\alpha_i^m\right]\left[\frac{\partial U_i}{\partial X^n}\alpha_j^n\right] \tag{6}$$

In the above equations, σ_k and σ_g are diffusion turbulent Prandtl numbers. And C_m, C_1, C_2 are turbulent modeling constants and are given in Table 1.

Method of Computation

Grid

This paper assumed that the geometry is symmetric in z-direction. 172×50×14 grid in x, y, z direction, respectively was used. A large number of grid is located near the moving band to consider wall effect of moving band.

In this study, the geometry is so complex that we used HyperMesh (1996) which is commercial package.

Discretisation

After the integral of the governing equations over the control volume, algebraic equations are obtained. Central differential scheme was used in the diffusion term, and upwind differential scheme was used in the convection term. Final form of the discretised equation (Peric, 1985) is

$$a_p\phi_p = \sum a_{nb}\phi_{nb} + C_p \tag{7}$$

where $a_m = a_m^c + a_m^{DN}$

$$a_p = \sum_n a_n^C + S_\phi''$$

$$C_P = S_f' + \left(\sum_l a_l^{DC}\phi_l^* + a_P^{DC}\phi_P^*\right) + \sum_n a_n^C\phi_n^*$$

m = E,W,N,S,T,B

n = EE,WW,NN,SS,TT,BB

l = E, W, N, S, T, B, NW, SE, SW, TE, TW, BE, BW, TN, TS, BN, BS

In the above equations, the ϕ^* are the values of the dependent variable ϕ obtained in the previous iteration.

Numerical analysis method

The equation (7) stores variables which is located in the main nodes (P,N,S,E,W,T,B) implicitly and stores variables which is located in the other nodes explicitly so the computing time is reduced. And final matrix is solved by SIP (Strongly Implicit Procedure) method. Non-staggered variable arrangement is used for all the variables to share the same control volume, which facilitates efficient computer programming. To avoid pressure oscillations which occurred by non-staggered arrangement, and to evaluate a velocity component at a cell face, we used the discretised momentum equations for the two neighboring nodes as the interpolation formulae, but replaced the terms representing pressure gradient across the cell face, by one which is centered about it (Rhie, 1981). Finally to calculate the pressure, SIMPLE algorithm was adopted in this paper.

Boundary condition

Inlet condition: In the present study, the inlet conditions are treated explicitly. In particular, special treatments are needed at the burner because the entrained velocity of burners should be specified in the computational domain. Any desired value of ϕ can be arranged to be the solution at an internal grid by setting source terms properly (Patankar, 1980).

Outlet condition: Neumann condition is applied to outlet condition. But suction's capacity is fixed, and suction has known velocity. So when suction is treated, Dirichilet condition is applied.

Wall condition: If the wall is fixed, no slip condition is applied. But if the wall is moving, no slip condition should be modified. The relative velocity components should replace the absolute velocity components in order to apply the moving effect in the shear stress expressions.

Symmetric condition: In z-direction, symmetric condition is applied.

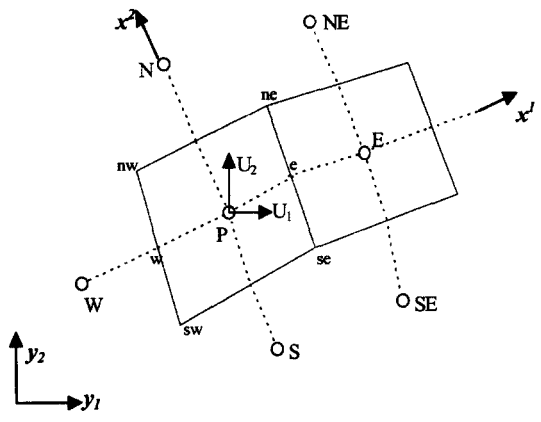

Fig. 2. Non-staggered variable arrangement.

Results and Discussions

The motivation for developing simulation model is to estimate the detailed thermal response of oven to thermal condition. To validate the simulation model, a base case was defined and its calculated results were compared with experimental data. The effects of parameters such as the velocity of the band and the capability of the suction on temperatures right above the band were studied.

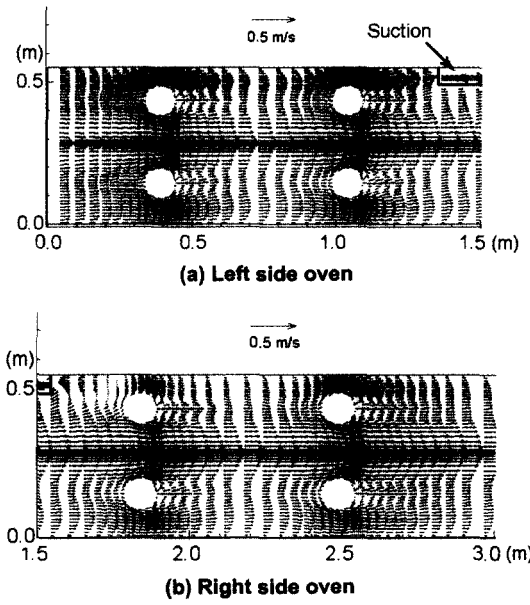

Fig. 3 Velocity vectors in the oven. (a) Velocity vectors, (b) Temperature distribution.

Tunnel oven used in this paper consists of 4 modules. All results of this paper are results in the second module.

The base case simulation

Figure 3-(a) shows the velocity vectors in the left side oven, and Fig. 3-(b) shows the velocity vectors in the right side oven. The base case oven is a 550 mm high× 1315 mm wide ×2880 mm deep tunnel oven equipped with 8 ribbon burners. Air enters the oven at 258°C with a constant velocity of 0.1 m/s. The band moves with 0.238 m/s velocity to the right and the suction expels air and ignition gas at 0.2 m/s. The burners exhaust the ignition gas with 0.123 m/s. Because of the suction, Fig. 3-(b) shows circulation behind the suction. However flow below the band is not too much affected by suction. Fig. 3-(a) shows increased velocity distribution before the suction and it is due to the alignment of suction duct flow and ignition gas. Also, we could see that the air in the oven is driven by the moving band.

Figure 4 shows yz-plane [lateral section cut: x=1.59 m] velocity and temperature distribution which is located behind the suction. Fig. 4-(a) shows the way how hot air below the band goes up to the suction. Fig. 4-(b) shows the temperature distribution. As shown in the Fig. 4-(b), the temperature at the side point of the band is higher than at the mid point of the band. It is because the hot air below the band goes up to the middle of band through oven side as shown in the Fig. 4-(a).

Figure 5 shows measured locations. They lie between band and burners in symmetric plane. K-type (Chromel-Alumel) thermocouples were used for temperature measurement. The thermometer is capable of measuring temperature of 3 points simultaneously and has three thermocouples in the stainless tube as shown in Fig. 6. Eight thermometers were used with 24 points temperature measured.

Figure 7-(a) shows comparison of experimental data and calculated result. In Fig. 7-(a) the burners are located at x=0.39 m, 1.04 m, 1.84 m, 2.49 m and suction is located at x=1.44 m. The temperature below the band was higher than the one above the band. Because moving band restricts the flow of the ignition gas from lower burners to suction. As shown in the Fig. 7-(a), calculated

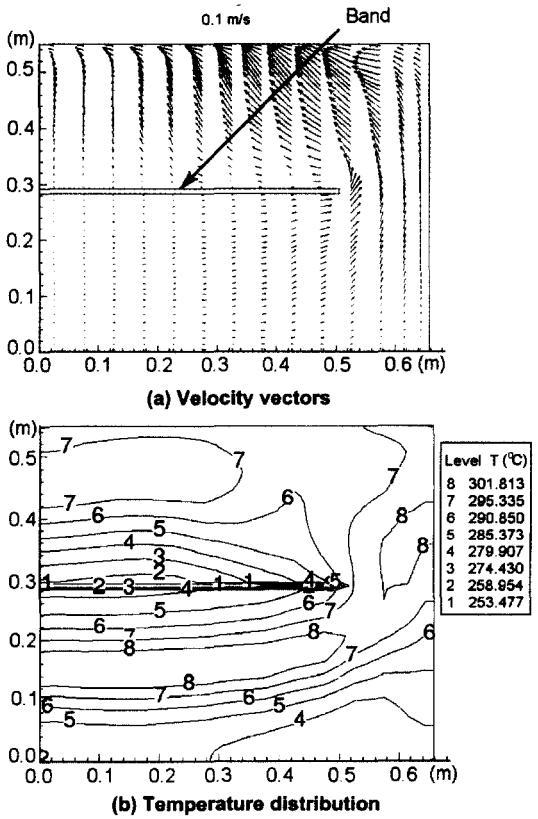

Fig. 4 Velocity vectors and temperature distribution of yz-plane at x=1.59 m.

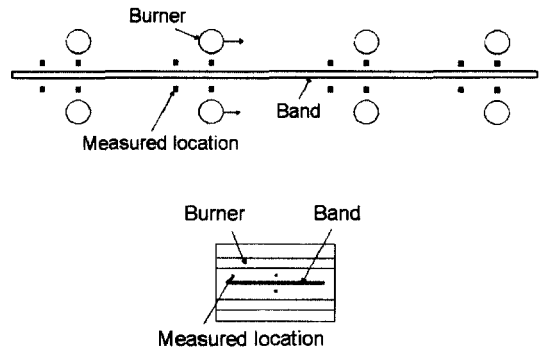

Fig. 5 Measured locations.

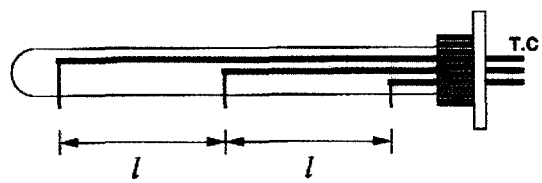

Fig. 6 Thermometer.

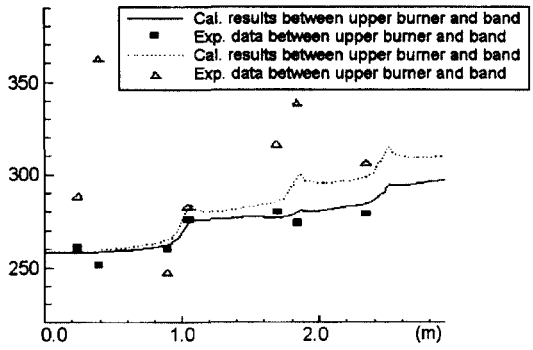

(a) Comparison of calculated results and experimental data

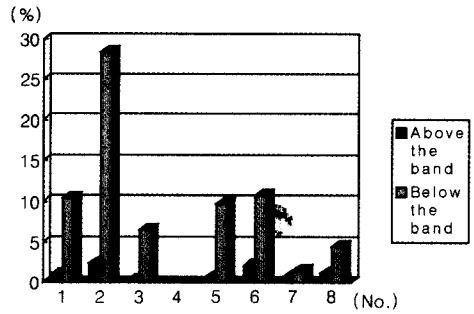

(b) Error of calculated results

Fig. 7 Comparison and error of calculated results and experimental data.

result and experimental data above the band are in good agreement. But the discrepancy between calculated result and experimental data below the band are quite large. This results from the assumptions that inlet air temperature and velocity is uniform, and the enclosure wall has a constant temperature.

Figure 7-(b) shows the error of calculated results. As shown in the Fig. 7-(b), the error of calculated result below the band is around 10% except the 2nd point.

Parametric study

Figure 8 shows temperature distribution above the band for the variation in band velocity. The band velocity, 0.238 m/s is actual industrial value. 0.475 m/s is double, 0.375 m/s is one and half and 0.119 m/s is half value of actual industrial value. As the band is faster, the temperature both at the mid point of the band and at the side point of the band increases. Because the faster band velocity gives the more convective heat transfer rates. But the magnitude of the increased temperature can be

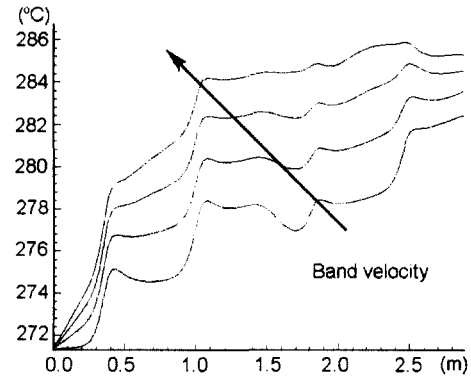

(a) Temperature at the mid point of the band (0.119 m/s, 0.238 m/s, 0.375 m/s, 0.475 m/s)

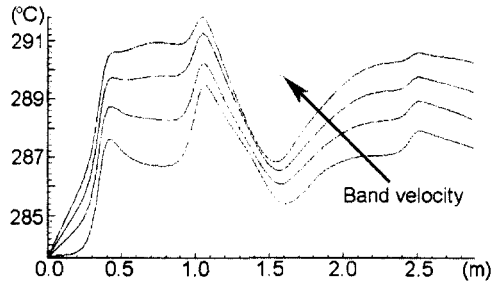

(b) Temperature at the side point of the band (0.119 m/s, 0.238 m/s, 0.375 m/s, 0.475 m/s)

Fig. 8 Temperature distribution with variation in band velocity.

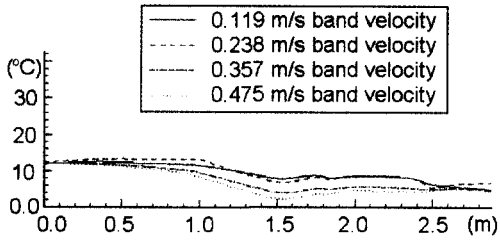

Fig. 9. Temperature difference between at the mid point of the band and the side point of the band with variation in band velocity.

ignored because increased temperature is about 1°C or 2°C.

Figure 9 shows the lateral temperature difference with the variation of band velocity. As was spoken, the temperature both at the mid point of the band and at the side point of the band increase, the lateral temperature difference is not affected by change of band velocity.

Figure 10 shows temperature distribution above the

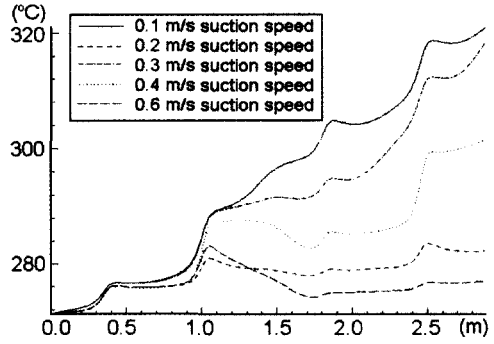

(a) Temperature at the mid point of the band

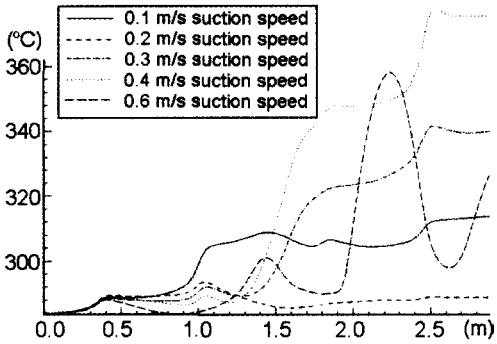

(b) Temperature at the side point of the band

Fig. 10 Temperature distribution with variation in suction velocity.

band for the variation in suction velocity. The band velocity, 0.2 m/s is actual industrial value. 0.6 m/s is three times, 0.4 m/s is double, 0.3 m/s is one and half and 0.1 m/s is half value of actual industrial value. As shown in Fig. 10, both temperature at the mid point of the band and at the side point of the band does not experience severe change from entrance to x=1m where suction is located. But after the x=1m, the temperature experiences severe temperature change.

The variation of suction velocity makes the small temperature difference at the mid point of the band about 4 °C in each case as shown at Fig. 10-(a).

But the variation of suction velocity makes the large temperature difference at the side point of the band, maximum 100°C, as shown at Fig. 10-(b). This is due to the fact that the hot air below the band gives heat to the side point of the band as shown in Fig. 4.

Figure 11 shows the lateral temperature difference with the variation of suction velocity. The lateral temperature difference is minimum when the suction velocity is 0.2 m/s. This velocity is the specific value when the suction flow rate equals with the ignition gas flow rate.

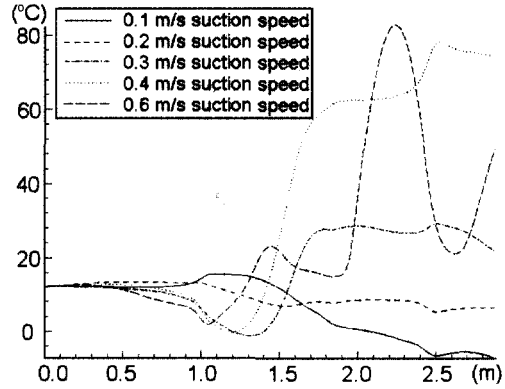

Fig. 11 Temperature difference between at the side point of the band and at the mid point of the band with the variation in suction velocity.

Fig. 11. Temperature difference between at the side point of the band and at the mid point of the band with the variation in suction velocity.

As previously mentioned, we should make lateral temperature difference small. By manipulating the suction flow rate, the lateral temperature difference can be reduced. But we should also consider the main function of suction, i.e., dispelling the ignition gas and moisture from biscuits.

Conclusions

Three dimensional numerical analysis performed here is capable of estimating the detailed temperature and velocity in the tunnel oven. The predicted results were feasible and showed the systems thermal response to variation in oven conditions.

The temperature at the side point of band is higher than the one at the mid point of band. Because the hot air below the band goes up to the mid point of band through oven side.

As the band is moving faster, the temperature both at the mid point of the band and at the side point of the band increase. But the magnitude of the increased temperature can be ignored because increased temperature is about 1°C or 2°C.

The change in suction velocity makes the lateral temperature difference so large that it is the most effective parameter on lateral temperature difference. The suction velocity 0.2 m/s maybe is the optimum velocity.

요 약

제빵용 터널오븐에 대한 수치해석을 하였다. 3차원, 정상, 비압축성, Navier-Stokes 방정식을 비엇갈림 변수 배열방법을 이용하여, 각각의 유한 체적에 적분하여 해석하였다. 수치해석적으로 얻어진 해를 시험값과 비교하여 정확도를 검증하였다. 밴드속도 및 배풍기 용량을 바꿔가며 계산하여, 각각의 변화가 터널오븐내의 온도장에 미치는 영향을 연구한 결과, 밴드의 이송속도를 온도차이에 영향을 거의 영향을 끼치지 못했으나, 배풍기 용량은 온도차이에 절대적인 영향을 끼쳤다.

References

Rhie C.M. 1981. *A numerical study of the flow past an isolated airfoil with separation.* Ph. D. Thesis, Dept. of Mech., University of Illinois at Urbana-Champagn, U.S.A.

Rho D.S., H.S. Ryou and K.G. Kang. 1997. *Development of computer design program for direct/indirect tunnel oven.* Final Report of CROWN Engineering.

Kang K.G., H.S. Ryou and Y.K. Choi. 1997. Numerical study of fluid flow and heat transfer in a tunnel oven. *The 5th Annual Conference of the Computational Fluid Dynamics Society of Canada,* May 25-27,1997,Victoria, Canada pp 8:17-8:22.

Patankar S.V. 1980. *Numerical heat transfer and fluid flow.* Hemisphere, Washing-ton D.C.

Peric M. 1985. *A finite volume method for the prediction of three-dimensional fluid flow in complex duct.* Ph. D.Thesis, Imperial College.

HyperMesh Documentation. 1996. Altair Computing, Inc.